Exploring the Thermodynamics of a Universal Fermi Gas

Sylvain Nascimbène, Nir Navon, Kaijun Jiang, Frédéric Chevy, Christophe Salomon

Exploring the thermodynamics of a universal Fermi gas

S. Nascimbène, N. Navon, K. J. Jiang, F. Chevy, and C. Salomon[1]
Laboratoire Kastler Brossel, CNRS,
UPMC, École Normale Supérieure,
24 rue Lhomond, 75231 Paris, France

(Dated: November 2, 2009)

PACS numbers: 03.75.Ss; 05.30.Fk; 32.30.Bv; 67.60.Fp

From sand piles to electrons in metals, one of the greatest challenges in modern physics is to understand the behavior of an ensemble of strongly interacting particles. A class of quantum many-body systems such as neutron matter and cold Fermi gases share the same universal thermodynamic properties when interactions reach the maximum effective value allowed by quantum mechanics, the so-called unitary limit [1, 2]. It is then possible to simulate some astrophysical phenomena inside the highly controlled environment of an atomic physics laboratory. Previous work on the thermodynamics of a two-component Fermi gas led to thermodynamic quantities averaged over the trap [3, 4, 5], making it difficult to compare with many-body theories developed for uniform gases. Here we develop a general method that provides for the first time the equation of state of a uniform gas, as well as a detailed comparison with existing theories [6, 7, 8, 9, 10, 11, 12, 13, 14]. The precision of our equation of state leads to new physical insights on the unitary gas. For the unpolarized gas, we prove that the low-temperature thermodynamics of the strongly interacting normal phase is well described by Fermi liquid theory and we localize the superfluid transition. For a spin-polarized system, our equation of state at zero temperature has a 2% accuracy and it extends the work of [15] on the phase diagram to a new regime of precision. We show in particular that, despite strong correlations, the normal phase behaves as a mixture of two ideal gases: a Fermi gas of bare majority atoms and a non-interacting gas of dressed quasi-particles, the fermionic polarons [10, 16, 17, 18].

In this letter we study the thermodynamics of a mixture of the two lowest spin states ($i = 1, 2$) of ^{6}Li prepared at a magnetic field $B = 834$ G (see Methods), where the dimensionless number $1/k_F a$ characterizing the s-wave interaction is equal to zero, the unitary limit. k_F is the Fermi momentum and a the scattering length. Understanding the universal thermodynamics at unitarity is a challenge for many-body theories because of the strong interactions between particles. Despite this complexity at the microscopic scale, all the macroscopic properties of an homogeneous system are encapsulated within a single equation of state $P(\mu_1, \mu_2, T)$ that relates the pressure P of the gas to the chemical potentials μ_i of the species i and to the temperature T. In the unitary limit, this relationship can be expressed as [1, 19, 20]

$$P(\mu_1, \mu_2, T) = P_1(\mu_1, T) h\left(\eta = \frac{\mu_2}{\mu_1}, \zeta = \exp\left(\frac{-\mu_1}{k_B T}\right)\right), \quad (1)$$

where $P_1(\mu_1, T) = -k_B T \lambda_{dB}^{-3}(T) f_{5/2}\left(-\zeta^{-1}\right)$ is the pressure of a single component non-interacting Fermi gas and $f_{5/2}(z) = \sum_{n=1}^{\infty} z^n/n^{5/2}$. $h(\eta, \zeta)$ is a universal function which contains all the thermodynamic information of the unitary gas (Fig.1). In cold atomic systems, the inhomogeneity due to the trapping potential makes the measurement of $h(\eta, \zeta)$ challenging.

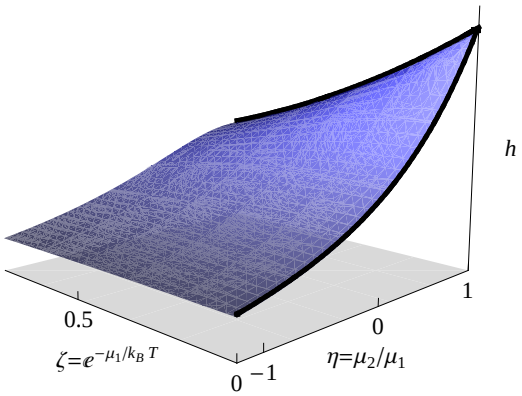

FIG. 1: Schematic representation of the universal function $h(\eta, \zeta)$ that fully describes the thermodynamics of the unitary gas as a function of chemical potential imbalance $\eta = \mu_2/\mu_1$ and of the inverse of the fugacity $\zeta = \exp(-\mu_1/k_B T)$. In this paper we measure the function h over the black lines $(1, \zeta)$ and $(\eta, 0)$ which correspond to the balanced unitary gas at finite temperature and to the spin-imbalanced gas at zero temperature, respectively.

We directly probe the local pressure of the trapped gas using *in situ* images, following the recent proposal [21]. In the local density approximation, the gas is locally homogeneous with local chemical potentials

$$\mu_i(\mathbf{r}) = \mu_i^0 - V(\mathbf{r}) \quad (2)$$

(μ_i^0 is the chemical potential at the bottom of the trap for species i). Then a simple formula relates the pressure P to the doubly-integrated density profiles

$$P(\mu_{1z}, \mu_{2z}, T) = \frac{m\omega_r^2}{2\pi}\left(\overline{n}_1(z) + \overline{n}_2(z)\right), \quad (3)$$

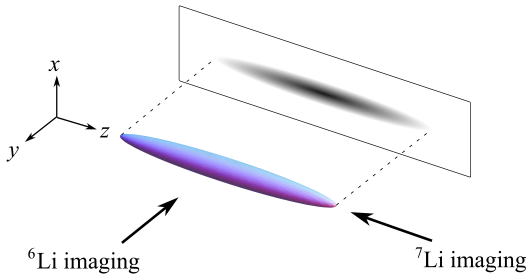

FIG. 2: The ^{6}Li atomic cloud is imaged in the direction y; the column density is then integrated along the direction x to give $\overline{n}(z)$. The ^{7}Li atoms are imaged after a time of flight along the z direction.

where $\overline{n}_i(z) = \int n_i(x,y,z)\mathrm{d}x\mathrm{d}y$, n_i being the atomic density. ω_r (resp. ω_z) is the transverse (resp. axial) angular frequency of a cylindrically symmetric trap (see Fig.2) and $\mu_{iz} = \mu_i(0,0,z)$ is the local chemical potential along the z axis. From a single image, we thus measure the equation of state (1) along the parametric line $(\eta,\zeta) = (\mu_{2z}/\mu_{1z}, \exp(-\mu_{1z}/k_BT))$, see below.

The interest of this method is straightforward. First, one directly measures the equation of state (EOS) of the uniform gas. Second, each pixel row z_i gives a point $h(\eta(z_i),\zeta(z_i))$ whose signal to noise ratio is essentially given by the one of $\overline{n}_1(z)+\overline{n}_2(z)$; typically one experimental run leads to ~ 100 points with a signal to noise between 3 and 10. With about 40 images one gets $\simeq 4000$ points $h(\eta,\zeta)$, which after averaging provides a low-noise EOS. The standard deviation, $\sigma = 2\%$, reveals new features of the EOS. In the following we illustrate the efficiency of our method on two important sectors of the parameter space (η,ζ) in Fig1: the balanced gas at finite temperature $(1,\zeta)$ and the zero-temperature imbalanced gas $(\eta,0)$.

The balanced unitary gas at finite temperature

We first measure the equation of state of the unpolarized unitary gas at finite temperature, $P(\mu_1,\mu_2,T) = P(\mu,T)$. The measurement of $h(1,\zeta)$ through the local pressure (3) can be done provided one knows the temperature T of the cloud and its central chemical potential μ^0.

• In the balanced case, model-independent thermometry is notoriously difficult because of the strong interactions. Inspired by [22], we overcome this issue by measuring the temperature of a ^{7}Li cloud in thermal equilibrium with the ^{6}Li mixture (see Methods).

• μ^0 is fitted on the hottest clouds so that the EOS agrees in the classical regime $\zeta \gg 1$ with the second-order virial expansion $h(1,\zeta) \simeq 2(1+\zeta^{-1}/\sqrt{2})$ [23]. For colder clouds we proceed recursively. The EOS of an image recorded at temperature T has some overlap with the previously determined EOS from all images with $T' > T$. In this overlap region μ_0 is fitted to minimize the distance between the two EOS's. This provides a new portion of the EOS at lower temperature. Using 40 images of clouds prepared at different temperatures, we thus reconstruct a low-noise EOS from the classical part down to the degenerate regime, as shown in Fig.3a.

We now comment the main features of the equation of state. At high temperature, the EOS can be expanded in powers of ζ^{-1} as a virial expansion [11]:

$$\frac{h(1,\zeta)}{2} = \frac{\sum_{k=1}^{\infty}\left((-1)^{k+1}k^{-5/2}+b_k\right)\zeta^{-k}}{\sum_{k=1}^{\infty}(-1)^{k+1}k^{-5/2}\zeta^{-k}},$$

where b_k is the k^{th} virial coefficient. Since we have $b_2 = 1/\sqrt{2}$ in the measurement scheme described above, our data provides for the first time the experimental values of b_3 and b_4. $b_3 = -0.35(2)$ is in excellent agreement with the recent calculation $b_3 = -0.291 - 3^{-5/2} = -0.355$ from [11] but not with $b_3 = 1.05$ from [12]. $b_4 = 0.096(15)$ involves the 4-fermion problem at unitarity and could interestingly be computed along the lines of [11].

Let us now focus on the low-temperature regime of the normal phase $\zeta_c < \zeta \ll 1$. In analogy with ^{3}He [24] or heavy-fermion metals [25], we fit our data with the EOS of a Landau Fermi liquid [26]:

$$P(\mu,T) = 2P_1(\mu,0)\left(\xi_n^{-3/2} + \frac{5\pi^2}{8}\xi_n^{-1/2}\frac{m^*}{m}\left(\frac{k_BT}{\mu}\right)^2\right), \quad (4)$$

$P_1(\mu,0) = 1/15\pi^2(2m/\hbar^2)^{3/2}\mu^{5/2}$ being the pressure of a single-component Fermi gas at zero temperature. m^* is the quasi-particle mass and ξ_n^{-1} is the compressibility of the normal gas extrapolated to zero temperature, and normalized to that of an ideal gas of same density. As seen in Fig.3b, from $T = T_c$ to $T = 0.8\mu/k_B$ the agreement with the data is excellent and we deduce two new parameters $m^*/m = 1.13(3)$ and $\xi_n = 0.51(2)$. Despite the strong interactions m^* is close to m, unlike the weakly interacting ^{3}He liquid for which $2.7 < m^*/m < 5.8$, depending on pressure [24]. Our ξ_n value is slightly lower than the variational Fixed-Node Monte-Carlo calculation $\xi_n = 0.56$ [10]. This yields the Landau parameters $F_0^s = \xi_n m^*/m - 1 = -0.42$ and $F_1^s = 3(m^*/m-1) = 0.39$ [26].

In the lowest temperature points (Fig.3c) we observe a sudden deviation of the data from the fit (4) at $(k_BT/\mu)_c = 0.32(3)$. We interpret this singular behavior as the transition from the normal phase to the superfluid phase. The error bar is dominated by our estimate of the systematic error introduced by the trap anharmonicity (see supplementary materials). This fundamental quantity has been extensively calculated in the recent years. Our value is in close agreement with the diagrammatic Monte-Carlo calculation $(k_BT/\mu)_c = 0.32(2)$ of [6] but differs from the self-consistent approach in [8] giving $(k_BT/\mu)_c = 0.41$, from the renormalization group prediction 0.24 in [27], from the Fixed-Node Monte-Carlo calculation 0.52(4) in [7], and from several other less precise theories. From equation (4) we deduce the total density $n = n_1 + n_2 = \partial P(\mu_i = \mu, T)/\partial\mu$ and the Fermi energy $E_F = k_BT_F = \hbar^2/2m(3\pi^2 n)^{2/3}$ at the transition point. We obtain $(\mu/E_F)_c = 0.49(2)$ and $(T/T_F)_c$=0.157(15), in very good agreement with [6]. Our measurement is the first direct determination of $(\mu/E_F)_c$ and $(T/T_F)_c$

in the homogeneous gas. It agrees with the extrapolated value of the MIT measurement [15].

Below T_c, advanced theories [7, 8] predict that $P(\mu,T)/2P_1(\mu,0)$ is nearly constant (Fig.3b). Therefore at $T=T_c$, $P/2P_1 \simeq \xi_s^{-3/2} \simeq 3.7$, and is consistent with our data. Here $\xi_s = 0.42(1)$ is the fundamental parameter characterizing the EOS of the balanced superfluid at zero temperature, a quantity extensively measured and computed in the recent years [2].

Our data is compared at all temperatures with the calculations from [6, 7, 8, 9] (Fig.3a). The agreement with [7] is very good for a large range of temperatures. However their determination of T_c was too high by about 60%. Concerning [6], the agreement on T_c is very good as mentioned above, but the deviation with our data is about one error bar of the Monte-Carlo method below $\zeta = 0.2$ and the deviation increases with temperature (Fig.3a). Furthermore, we show in the supplementary material that $h(1,\zeta)/2$ must be greater than 1, an inequality violated by the two hottest Monte-Carlo points of [6].

From our homogeneous EOS we can deduce the equation of state of the harmonically trapped unitary gas by integrating $h(1,\zeta)$ over the trap (see supplementary material). In particular, we find a critical temperature for the trapped gas $(T/T_F)_c = 0.19(2)$, where $T_F = \hbar(3\omega_r^2\omega_z N)^{1/3}$. This value agrees very well with the recent measurement of [28], and with less precise measurements [5, 29, 30] but differs from [4, 31].

The zero-temperature imbalanced unitary gas

Let us now explore a second line in the universal diagram $h(\eta,\zeta)$ (Fig.1) by considering the case of the $T=0$ spin-imbalanced mixture $\mu_2 \neq \mu_1$, *i.e.* $\eta \neq 1$. Previous work [18, 32, 33] has shown that phase separation occurs in a trap. Below a critical population imbalance a fully-paired superfluid occupies the center of the trap. It is surrounded by a normal mixed phase and an outer rim consisting of an ideal gas of the majority component. In two out of the three previous experiments including ours [18, 32], the local density approximation has been carefully checked. We are therefore entitled to use (3) to analyze our data.

As in the previous case, the relationship between the pressure and the EOS requires the knowledge of the chemical potentials μ_1^0 and μ_2^0 at the center of the trap.

- μ_1^0 is determined using the outer shell of the majority spin component ($i=1$). The pressure profile $P(\mu_{1z},\mu_{2z},0)$ corresponds to the Fermi-Dirac distribution and is fitted with the Thomas-Fermi formula $P_1 = \alpha(1-z^2/R_1^2)^{5/2}$, providing $\mu_1^0 = \frac{1}{2}m\omega_z^2 R_1^2$. Using P_1 for the calculation of $h = P/P_1$ cancels many systematic effects on the absolute value of the pressure.
- μ_2^0 is fitted by comparison in the superfluid region with the superfluid equation of state at zero temperature [19]:

$$h(\eta,0) = (1+\eta)^{5/2}/(2\xi_s)^{3/2}. \qquad (5)$$

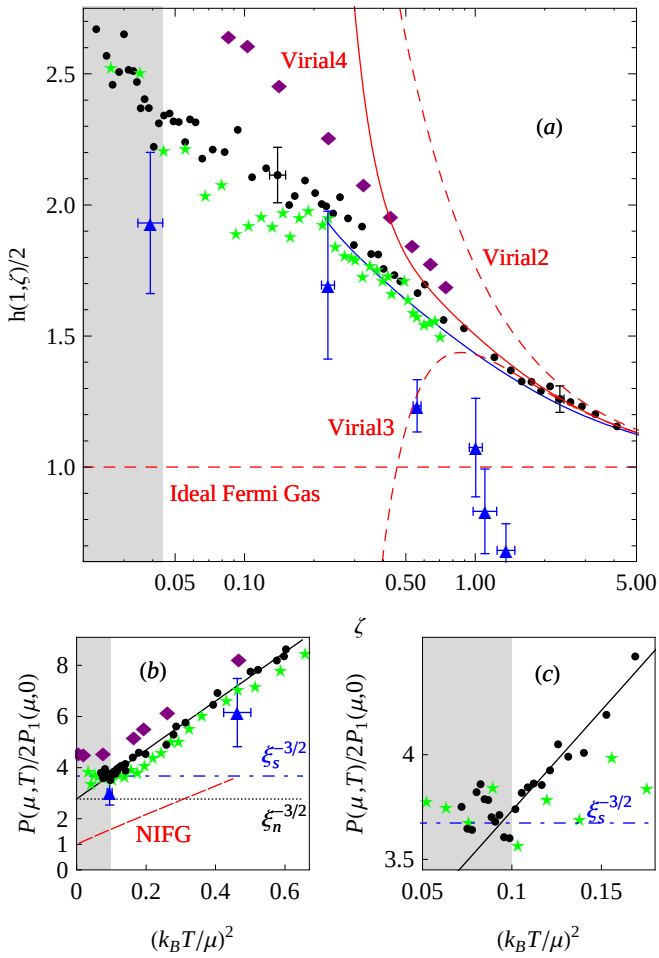

FIG. 3: (color online) (a) Finite-temperature equation of state $h(1,\zeta)$ of a balanced unitary Fermi gas (black dots). The error bars represented at $\zeta = 0.14$ and $\zeta = 2.3$ indicate the 5% accuracy of our EOS. The red curves are the successive virial expansions up to 4$^{\text{th}}$ order. The blue triangles are from [6], the green stars from [7], the purple diamonds from [8], and the blue solid line from [9]. The grey region indicates the superfluid phase. (b) Equation of state $P(\mu,T)/P(\mu,0)$ as a function of $(k_BT/\mu)^2$, fitted by the Fermi liquid equation of state (4). The red dashed line is the non-interacting Fermi gas (NIFG). The horizontal dot-dashed (resp. dotted) line indicates the zero-temperature pressure of the superfluid phase $\propto \xi_s^{-3/2}$ (resp. normal phase $\propto \xi_n^{-3/2}$). (c) Expanded view of (b) near T_c. The sudden deviation of the data from the fit occurs at $(k_BT/\mu)_c = 0.32(3)$ that we interpret as the superfluid transition.

Our measured equation of state $h(\eta,0)$ is displayed in Fig.4. By construction our data agrees for $\eta \gtrsim 0.1$ with eq.(5). In Fig.4 the slope of $h(\eta,0)$ displays an obvious discontinuity for $\eta = \eta_c = 0.065(20)$. This is a signature of a first-order quantum phase transition to the partially polarized normal phase. The error bar is dominated by the uncertainty on ξ_s. This value is slightly higher than the prediction $\eta_c = 0.02$ given by the fixed-node Monte-Carlo [10] and than the value $\eta_c = 0.03(2)$ measured in [15].

From the relations $n_i = \partial P/\partial\mu_i$ we deduce from $h(\eta,0)$

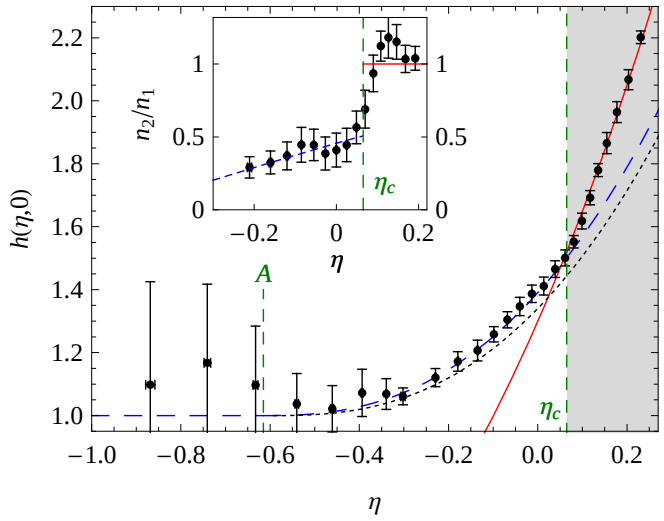

FIG. 4: (color online) Equation of state of the zero-temperature imbalanced unitary gas $h(\eta, 0)$ (black dots). The red solid line is the superfluid equation of state, the blue dashed line is the ideal Fermi liquid equation (6) with $A = -0.615$, $m^* = 1.20m$ and the black dotted line is the Monte Carlo calculation from [10]. Inset: Local density ratio n_2/n_1 as a function of η. The red solid line $n_2/n_1 = 1$ corresponds to the fully paired superfluid and blue dashed line to the model (6).

the density ratio n_2/n_1 (see inset in Fig.4) This ratio is discontinuous at the phase transition, from a maximum value in the normal phase $(n_2/n_1)_c = 0.5(1)$ to $n_2 = n_1$ in the superfluid phase. This discontinuity is strongly temperature-dependent as it vanishes at the tricritical point $T = 0.07T_F$ [15]. Our value is close to the zero-temperature calculation 0.44 [10] and agrees with the coldest MIT samples, at $k_BT \simeq 0.03\mu_1^0$. This justifies our $T = 0$ assumption made above.

For $\eta < \eta_c$ our equation of state $h(\eta, 0)$ lies slightly above the variational fixed-node Monte Carlo calculation [10]. This difference is clearly revealed by the high accuracy (2% in the normal phase) resulting from our analysis method.

Our data displays a better agreement with a simple polaron model. A polaron is a quasi-particle describing a single minority atom immersed in the majority Fermi sea [16, 17, 18]. It is characterized by a renormalized chemical potential $\mu_2 - A\,\mu_1$ and an effective mass m_p^*. For a mixture of a Fermi sea and an ideal gas of polarons, equation (1) can be written as

$$h(\eta, 0) = 1 + \left(\frac{m_p^*}{m}\right)^{3/2} (\eta - A)^{5/2}. \qquad (6)$$

A and m_p^* have recently been calculated exactly [14]: $A = -0.615$, $m_p^*/m = 1.20(2)$ and with these values inserted in (6) the agreement with our data is perfect. We therefore conclude that interactions between polarons are not visible at this level of precision.

Alternatively, we can fit our data with m_p^*/m as a free parameter in (6). We obtain $m_p^*/m = 1.20(2)$. The uncertainty combines the standard error of the fit and the uncertainty on ξ_s. This value agrees with our previous measurement $m_p^*/m = 1.17(10)$ [18] (with a 5-fold improvement in precision), with the theoretical value $m_p^*/m = 1.20(2)$ in [14] and with the variational calculation [13]. It differs from the values 1.09(2) in [34], 1.04(3) in [10], and from the experimental value 1.06 in [35].

b_3	b_4	$(k_BT/\mu)_c$	$(\mu/E_F)_c$	$(T/T_F)_c$
-0.35(2)	0.096(15)	0.32(3)	0.49(2)	0.157(15)
ξ_n	m^*/m	η_c	$(n_2/n_1)_c$	m_p^*/m
0.51(2)	1.13(3)	0.065(20)	0.5(1)	1.20(2)

TABLE I: Table of quantities measured in this work.

We arrive at a simple physical picture of the $T = 0$ spin-polarized gas: the fully paired superfluid is described by an ideal gas EOS renormalized by a single coefficient ξ_s; the normal phase is nothing but two ideal gases, one of bare majority particles and one of polaronic quasi-particles.

In conclusion, we have introduced a powerful method for the measurement of the equation of state of the unitary and homogeneous Fermi gas, that enables direct comparison with theoretical models and provides a set of new parameters shown in Tab.I. The method can readily be extended to any multi-component cold atom gas in three dimensions that fulfills the local density approximation (see supplementary discussion). We have shown that the unitary Fermi gas is a high-T_c system whose normal phase is well described by Fermi liquid theory, unlike high-T_c cuprates.

Methods

Our experimental setup is presented in [18]. We load into a mixed magneto-optical trap and evaporate a mixture of ^{6}Li in the $|1/2, \pm 1/2\rangle$ states and of ^{7}Li in the $|1, 1\rangle$ state at 834 G. The cloud typically contains $N_6 = 5$ to 10×10^4 ^{6}Li atoms in each spin state and $N_7 = 5$ to 20×10^3 ^{7}Li atoms at a temperature $T \sim 100$ nK. The ^{6}Li trap frequencies are $\omega_z/2\pi = 37$ Hz, $\omega_r/2\pi \sim 1$ kHz (Fig.2). ^{6}Li atoms are imaged *in situ* using absorption imaging, while ^{7}Li atoms are imaged after time of flight, providing the temperature in the same experimental run. Since the scattering length describing the interaction between ^{7}Li and ^{6}Li atoms, $a_{67} = 2$ nm, is much smaller than k_F^{-1}, the ^{7}Li thermometer has no influence on the ^{6}Li density profiles. The ^{7}Li-^{6}Li collision rate, $\Gamma_{67} = 10\ \mathrm{s}^{-1}$, is large enough to ensure thermal equilibrium between the two species. As the scattering length between the ^{7}Li atoms, $a_{77} = -3$ nm is negative, the cloud becomes unstable when a BEC forms. This sets a limit to our lowest temperatures. For this reason, for the measurement of the zero-temperature equation of state of the imbalanced gas, we do not use ^{7}Li thermometry.

[1] Ho, T. Universal thermodynamics of degenerate quantum gases in the unitarity limit. *Phys. Rev. Lett.* **92**, 90402 (2004).

[2] Inguscio, M., Ketterle, W. & Salomon, C. Ultracold Fermi Gases. *Proceedings of the International School of Physics Enrico Fermi, Course CLXIV, Varenna* (2006).

[3] Stewart, J., Gaebler, J., Regal, C. & Jin, D. Potential Energy of a ^{40}K Fermi Gas in the BCS-BEC Crossover. *Phys. Rev. Lett.* **97**, 220406 (2006).

[4] Luo, L., Clancy, B., Joseph, J., Kinast, J. & Thomas, J. Measurement of the entropy and critical temperature of a strongly interacting Fermi gas. *Phys. Rev. Lett.* **98**, 80402 (2007).

[5] Luo, L. & Thomas, J. Thermodynamic Measurements in a Strongly Interacting Fermi Gas. *J. Low Temp. Phys.* **154**, 1–29 (2009).

[6] Burovski, E., Prokofev, N., Svistunov, B. & Troyer, M. Critical temperature and thermodynamics of attractive fermions at unitarity. *Phys. Rev. Lett.* **96**, 160402 (2006).

[7] Bulgac, A., Drut, J. & Magierski, P. Spin 1/2 fermions in the unitary regime: A superfluid of a new type. *Physical review letters* **96**, 90404 (2006).

[8] Haussmann, R., Rantner, W., Cerrito, S. & Zwerger, W. Thermodynamics of the BCS-BEC crossover. *Phys. Rev. A* **75**, 23610 (2007).

[9] Combescot, R., Alzetto, F. & Leyronas, X. Particle distribution tail and related energy formula. *Phys. Rev. A* **79**, 053640 (2009).

[10] Lobo, C., Recati, A., Giorgini, S. & Stringari, S. Normal state of a polarized Fermi gas at unitarity. *Phys. Rev. Lett.* **97**, 200403 (2006).

[11] Liu, X., Hu, H. & Drummond, P. Virial expansion for a strongly correlated Fermi gas. *Phys. Rev. Lett.* **102**, 160401 (2009).

[12] Rupak, G. Universality in a 2-Component Fermi System at Finite Temperature. *Phys. Rev. Lett.* **98**, 90403 (2007).

[13] Combescot, R., Recati, A., Lobo, C. & Chevy, F. Normal state of highly polarized Fermi gases: simple many-body approaches. *Phys. Rev. Lett.* **98**, 180402 (2007).

[14] Combescot, R. & Giraud, S. Normal state of highly polarized Fermi gases: full many-body treatment. *Phys. Rev. Lett.* **101**, 050404 (2008).

[15] Shin, Y., Schunck, C., Schirotzek, A. & Ketterle, W. Phase diagram of a two-component Fermi gas with resonant interactions. *Nature* **451**, 689–693 (2008).

[16] Chevy, F. Universal phase diagram of a strongly interacting fermi gas with unbalanced spin populations. *Phys. Rev. A* **74**, 063628 (2006).

[17] Schirotzek, A., Wu, C.-H., Sommer, A. & Zwierlein, M. W. Observation of fermi polarons in a tunable fermi liquid of ultracold atoms. *Phys. Rev. Lett.* **102**, 230402 (2009).

[18] Nascimbene, S. *et al.* Collective Oscillations of an Imbalanced Fermi Gas: Axial Compression Modes and Polaron Effective Mass. *Phys. Rev. Lett.* **103**, 170402 (2009).

[19] Chevy, F. Density profile of a trapped strongly interacting Fermi gas with unbalanced spin populations. *Phys. Rev. Lett.* **96**, 130401 (2006).

[20] Bulgac, A. & McNeil Forbes, M. Zero temperature thermodynamics of asymmetric fermi gases at unitarity. *Phys. Rev. A* **75** (2007).

[21] Ho, T. & Zhou, Q. Obtaining phase diagram and thermodynamic quantities of bulk systems from the densities of trapped gases. *arXiv:0901:0018* (2009).

[22] Spiegelhalder, F. *et al.* Collisional Stability of ^{40}K Immersed in a Strongly Interacting Fermi Gas of ^{6}Li. *arXiv:0908.1101* (2009).

[23] Ho, T. & Mueller, E. High temperature expansion applied to fermions near Feshbach resonance. *Phys. Rev. Lett.* **92**, 160404 (2004).

[24] Greywall, D. S. Specific heat of normal liquid ^{3}He. *Phys. Rev. B* **27**, 2747–2766 (1983).

[25] Stewart, G. Heavy-fermion systems. *Rev. Mod. Phys.* **56**, 755–787 (1984).

[26] Pines, D. & Nozieres, P. *The Theory of Quantum Liquids, vol. I: Normal Fermi Liquids* (WA Benjamin, New York, 1966).

[27] Gubbels, K. & Stoof, H. Renormalization group theory for the imbalanced Fermi gas. *Phys. Rev. Lett.* **100**, 140407 (2008).

[28] Riedl, S., Guajardo, E., Kohstall, C., Denschlag, J. & Grimm, R. Superfluid Quenching of the Moment of Inertia in a Strongly Interacting Fermi Gas. *arXiv:0907.3814* (2009).

[29] Greiner, M., Regal, C. & Jin, D. Emergence of a molecular Bose-Einstein condensate from a Fermi gas. *Nature* **426**, 537–540 (2003).

[30] Inada, Y. *et al.* Critical temperature and condensate fraction of a fermion pair condensate. *Phys. Rev. Lett.* **101**, 180406 (2008).

[31] Kinast, J. *et al.* Heat capacity of a strongly interacting Fermi gas. *Science* **307**, 1296 (2005).

[32] Shin, Y., Zwierlein, M., Schunck, C., Schirotzek, A. & Ketterle, W. Observation of phase separation in a strongly interacting imbalanced Fermi gas. *Phys. Rev. Lett.* **97**, 30401 (2006).

[33] Partridge, G., Li, W., Kamar, R., Liao, Y. & Hulet, R. Pairing and phase separation in a polarized Fermi gas. *Science* **311**, 503–505 (2006).

[34] Pilati, S. & Giorgini, S. Phase separation in a polarized Fermi gas at zero temperature. *Phys. Rev. Lett.* **100**, 030401 (2008).

[35] Shin, Y. Determination of the equation of state of a polarized fermi gas at unitarity. *Phys. Rev. A* **77**, 041603 (2008).

[36] Feynman, R. Statistical Mechanics: A set of lectures. *Frontiers in Physics. New York* (1972).

Supplementary Discussion
Equation of State of the Trapped Unitary Gas

In this work, we have measured the equation of state of the homogeneous unitary gas. We can deduce from our data the EOS of the trapped balanced unitary gas, which has been measured in [3, 5].

Using the local density approximation, the total atom number $N = \int n\,\mathrm{d}r^3$ is expressed as a function of the temperature T and the chemical potential μ^0 at the center, involving the function $h(1,\zeta)$:

$$N = \frac{-2}{\sqrt{\pi}}\left(\frac{k_B T}{\hbar\omega}\right)^3 \int_{\zeta_0}^{\infty} \frac{\mathrm{d}\log^{1/2}(\zeta/\zeta_0)}{\mathrm{d}\zeta} f_{5/2}(-\zeta^{-1}) h(\zeta)\mathrm{d}\zeta, \tag{7}$$

where $\zeta_0 = \exp(-\mu^0/k_B T)$ and $\omega = (\omega_r^2\omega_z)^{1/3}$. We use for the calculation a discretized version of (7) taken solely on our experimental values of h, *i.e.* without using any interpolating or fitting function. Similar ex-

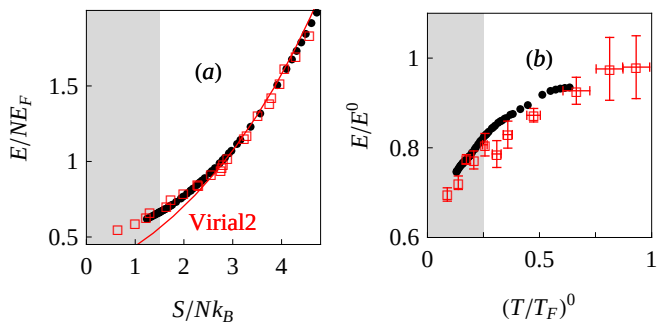

FIG. 5: (color online) (a) Comparison between our equation of state of the trapped unitary gas E/NE_F as a function of S/Nk_B (in black) and the EOS measured in [5] (in red). The red curve is the second-order virial equation of state. (b) Comparison between our EOS E/E^0 as a function of $(T/T_F)^0$ (in black) and the EOS measured on ^{40}K in [3] (in red). The grey regions correspond to the superfluid phase.

pressions are used to calculate the Fermi temperature $E_F = k_B T_F = \hbar\omega(3N)^{1/3}$, the total entropy S and energy E of the cloud. The equation of state E/NE_F as a function of S/Nk_B, displayed in (Fig.5a), is in very good agreement with [5].

The normal-superfluid phase transition for the trapped gas occurs when at the trap center $\zeta_0 = \zeta_c = \exp(-(k_B T/\mu)_c^{-1})$, with $(k_B T/\mu)_c = 0.32(3)$, as measured on the homogeneous EOS $h(1,\zeta)$. At this point we get $(T/T_F)_c = 0.19(2)$, $(S/Nk_B)_c = 1.5(1)$ and $(E/NE_F)_c = 0.67(5)$.

In order to make the comparison with [3], we also express the equation of state E/E^0 as a function of $(T/T_F)^0$, where the superscript ^{0} refers to the quantities evaluated on a non-interacting Fermi gas having the same entropy (Fig.5b). The good agreement with the measurement in [3], performed on ^{40}K clouds, illustrates the universality of the unitary gas.

Trap Anharmonicity

First, in the axial direction z, the confinement is produced magnetically and the corresponding anharmonicity is negligible. In the radial direction, we develop the gaussian potential to fourth order around $\rho = 0$:

$$V_r(\rho) = V_0\left(1 - \exp\frac{-\rho^2}{\sigma^2}\right) \simeq \frac{1}{2}m\omega_r^2\rho^2 + \epsilon\rho^4,$$

where $m\omega_r^2 = 2V_0/\sigma^2$ and $\epsilon = -V_0/2\sigma^4$. In the balanced case, we have

$$\overline{n}(z) = \int \mathrm{d}^2\rho\, n\left(\mu^0 - \frac{1}{2}m\omega_z^2 z^2 - \frac{1}{2}m\omega_r^2\rho^2 - \epsilon\rho^4\right).$$

Introducing $n = \partial P/\partial\mu$ and defining $u = m\omega_r^2\rho^2/2 + \epsilon\rho^4$ we obtain, to lowest order,

$$\frac{m\omega_r^2}{2\pi}\overline{n}(z) = P(\mu_z) + \int_0^\infty P(\mu_z - u)\frac{\mathrm{d}u}{V_0}.$$

The error on the measurement of h is then

$$\frac{m\omega_r^2\,\overline{n}(z)}{2\pi P_1(\mu_z,T)} - h(1,\zeta) = \frac{k_B T}{V_0}\int_\zeta^\infty \frac{f_{5/2}(-\zeta'^{-1})}{f_{5/2}(-\zeta^{-1})}\frac{h(1,\zeta')}{\zeta'}\mathrm{d}\zeta'. \quad (8)$$

We evaluate the integral in (8) using the experimental values of $h(1,\zeta)$. In our shallowest trap, the worst case anharmonicity effect is 5%. The very good agreement between the experimental value $b_3 = -0.35(2)$ and the theoretical value $b_3 = -0.355$ of the third virial coefficient indicates no other systematic error higher than 6%. From this error we deduce a 10% uncertainty on the value of $(k_B T/\mu)_c$.

An exact inequality on the equation of state of an attractive Fermi gas

Writing the hamiltonian as $\widehat{H} = \widehat{H}_0 + \widehat{U}$, where $\widehat{H}_0$ is the single-particle part of the hamiltonian and $\widehat{U}$ is the inter-particle interaction, one has the general inequality $\Omega \leq \Omega_0 + \langle V\rangle_0$, where Ω_0 is the grand potential associated with $\widehat{H}_0$ and $\langle\cdot\rangle_0$ is the thermal average related to $\widehat{H}_0$ [36]. Taking for U a short range square potential of depth $U_0 < 0$ recovering the true scattering length, one has trivially $\langle\widehat{V}\rangle_0 < 0$, hence $\Omega \leq \Omega_0$. Using the thermodynamic identity $\Omega = -PV$, and recalling that $\Omega_0 = -2P_1 V$ and $h = P/P_1$, we finally get the inequality

$$h(1,\zeta) \geq 2.$$

Extension to a Multi-Component System

We extend the equation (2) to a mixture of species i, of mass m_i, trapped in a harmonic trap of transverse frequencies ω_{ri}, following the calculations in [21]. Using Gibbs-Duhem relation at a constant temperature T, $\mathrm{d}P = \sum_i n_i \mathrm{d}\mu_i$, then

$$\sum_i \frac{m_i\omega_{ri}^2}{2\pi}\overline{n}_i = \int\sum_i \frac{m_i\omega_{ri}^2}{2\pi}\mathrm{d}x\mathrm{d}y\frac{\partial P}{\partial\mu_i} = \int\sum_i \mathrm{d}\mu_i\frac{\partial P}{\partial\mu_i},$$

where we have used local density approximation (2) to convert the integral over space to an integral on the chemical potentials. The integral is straightforward and yields to

$$P(\mu_{iz},T) = \frac{1}{2\pi}\sum_i m_i\omega_{ri}^2\overline{n}_i(z).$$

Acknowledgements We are grateful to R. Combescot, X. Leyronas, and T. Giamarchi for fruitful discussions on Fermi liquid theory, C. Cohen-Tannoudji, F. Gerbier, and G. Shlyapnikov for critical reading of the manuscript. We acknowledge support from ESF (Euroquam), SCALA, ANR FABIOLA, Région Ile de France (IFRAF), ERC and Institut Universitaire de France.

Correspondence S. Nascimbène and N. Navon contributed equally to this work. Correspondence and requests for materials should be addressed to S. N. (email: sylvain.nascimbene@ens.fr).